NeuroImage: Clinical 20 (2018) 347–356

Contents lists available at ScienceDirect

NeuroImage: Clinical

journal homepage: www.elsevier.com/locate/ynicl

Connecting occipital alpha band peak frequency, visual temporal resolution, and occipital GABA levels in healthy participants and hepatic encephalopathy patients

Thomas J. Baumgarten[a,b,*], Julia Neugebauer[a], Georg Oeltzschner[c,d], Nur-Deniz Füllenbach[e], Gerald Kircheis[e], Dieter Häussinger[e], Joachim Lange[a], Hans-Jörg Wittsack[f], Markus Butz[a], Alfons Schnitzler[a]

[a] Institute of Clinical Neuroscience and Medical Psychology, Medical Faculty, Heinrich Heine University Düsseldorf, 40225 Düsseldorf, Germany
[b] Neuroscience Institute, New York University Langone Medical Center, New York, NY, USA
[c] Russell H. Morgan Department of Radiology and Radiological Science, The Johns Hopkins University School of Medicine, Baltimore, MD, USA
[d] F.M. Kirby Center for Functional Brain Imaging, Kennedy Krieger Institute, Baltimore, MD, USA
[e] Department of Gastroenterology, Hepatology and Infectiology, Medical Faculty, Heinrich Heine University Düsseldorf, 40225 Düsseldorf, Germany
[f] Department of Diagnostic and Interventional Radiology, Medical Faculty, Heinrich Heine University Düsseldorf, 40225 Düsseldorf, Germany

ARTICLE INFO

Keywords:
Hepatic encephalopathy
Magnetoencephalography
Alpha oscillations
Peak frequency
Magnetic resonance spectroscopy
GABA

ABSTRACT

Recent studies have proposed a connection between the individual alpha band peak frequency and the temporal resolution of visual perception in healthy human participants. This connection rests on animal studies describing oscillations in the alpha band as a mode of phasic thalamocortical information transfer for low-level visual stimuli, which critically relies on GABAergic interneurons.

Here, we investigated the interplay of these parameters by measuring occipital alpha band peak frequency by means of magnetoencephalography, visual temporal resolution by means of behavioral testing, and occipital GABA levels by means of magnetic resonance spectroscopy. Importantly, we investigated a sample of healthy participants and patients with varying grades of hepatic encephalopathy, which are known to exhibit decreases in the investigated parameters, thus providing an increased parameter space.

We found that occipital alpha band peak frequency and visual temporal resolution were positively correlated, i.e., higher occipital alpha band peak frequencies were on average related to a higher temporal resolution. Likewise, occipital alpha band peak frequency correlated positively with occipital GABA levels. However, correlations were significant only when both healthy participants and patients were included in the analysis, thereby indicating a connection of the measures on group level (instead of the individual level). These findings provide new insights into neurophysiological and neurochemical underpinnings of visual perception.

1. Introduction

Neuronal oscillatory activity has received increasing attention within the neuroscientific community during the last two decades (Buzsáki and Draguhn, 2004). Neuronal oscillations presumably represent a dynamic functional link for neuronal communication. In this role, neuronal oscillations are centered between the relatively invariant dimension of anatomical connections on the one side and the highly flexible dimension of behavioral output on the other side (Buzsáki and Watson, 2012; Singer and Lazar, 2016). Historically, the brain was interpreted as operating in a passive stimulus-driven mode substantially focused on bottom-up serial processing of stimulus properties (e.g., Hubel and Wiesel, 1965; Thorpe et al., 1996). In contrast, current theories emphasize the role of dynamic internal brain states which affect stimulus processing in a largely stimulus-independent top-down direction. In this context, neuronal oscillations are considered to be

Abbreviations: CFF, Critical flicker frequency; CSD, Cross-spectral density; EC, Eyes-closed; ECG, Electro-cardiogram; EO, Eyes-open; EOG, Electro-oculogram; GABA, γ-aminobutyric acid; GABA+/Cr, GABA-to creatine -ratio; HE, Hepatic encephalopathy; HE1, Clinically manifest HE grade 1; HPI, Head position indication; ICA, Independent component analysis; MEG, Magnetoencephalography; mHE, Minimal HE; MNI, Montreal Neurological Institute; MRS, Magnetic resonance spectroscopy

* Corresponding author at: Neuroscience Institute, New York University Langone Medical Center, New York, NY, USA.
E-mail address: Thomas.Baumgarten@nyumc.org (T.J. Baumgarten).

https://doi.org/10.1016/j.nicl.2018.08.013
Received 8 March 2018; Received in revised form 24 July 2018; Accepted 8 August 2018
Available online 09 August 2018

critical for the implementation of top-down processes (Engel et al., 2001; Hipp et al., 2011).

The functional impact of neuronal oscillations is specifically well documented for the alpha band (~7–14 Hz, Haegens et al., 2014). Alpha band oscillations are most prominent in parieto-occipital cortex areas (Hari et al., 1997) and are both predictive (Hanslmayr et al., 2007; van Dijk et al., 2008) and causally relevant (Romei et al., 2010) for neuronal processing and perception of visual stimuli. Mechanistically, the connection between cortical alpha band oscillations and visual stimulus perception rests on the synchronization of alpha band oscillations to periodic activity in thalamic relay neurons (Lőrincz et al., 2009). Thus, alpha band oscillations likely reflect a mode of phasic information transfer within a thalamocortical network (Bollimunta et al., 2011; Vijayan and Kopell, 2012). This phasic pattern relies heavily on pulsed inhibition mediated by GABAergic interneurons (Lőrincz et al., 2009). Both the phasic patterns of information transfer as well as the alpha cycle length predetermine alpha band activity to shape the temporal structure of perception (Busch et al., 2009; Mathewson et al., 2009).

This temporal dimension of perception is closely linked to the concept of perceptual cycles (Varela et al., 1981; Vanrullen and Koch, 2003; Vanrullen, 2016; Baumgarten et al., 2015; Baumgarten et al., 2017). Perceptual cycles constitute discrete temporal windows for neuronal stimulus processing, which temporally sample incoming stimuli. While experimental evidence for this concept and its connection to oscillatory alpha band activity has been first provided by a seminal study of Varela et al. (1981), multiple attempts to replicate this finding have remained unsuccessful (see Vanrullen and Koch, 2003; Vanrullen et al., 2014). Nonetheless, recent findings demonstrate that perceptual sampling of visual stimuli is primarily determined by the frequency of individual alpha band activity (Dugué et al., 2011; Chakravarthi and Vanrullen, 2012; Cecere et al., 2015; Samaha and Postle, 2015). Some studies aimed to connect individual markers of alpha band activity to individual perceptual performance levels. Such approaches targeting individual oscillatory parameters mostly focus on the peak frequency of a specific predetermined frequency band. Here, peak frequency is defined as the specific frequency within a predefined band exhibiting the highest spectral power (i.e., the power-dominant frequency). Recent studies reported correlations between the individual alpha band peak frequency and the speed of temporal sampling in the visual (Samaha and Postle, 2015) and audio-visual domain (Cecere et al., 2015). The theory of perceptual cycles and the abovementioned findings provide the hypothesis of a positive linear correlation between alpha band peak frequency and visual temporal resolution. Individuals with a low alpha band peak frequency should exhibit a low visual temporal resolution. However, testing this hypothesis is hindered because, in healthy subjects, alpha band peak frequencies are distributed only across a limited range (Haegens et al., 2014). Therefore, it can be beneficial to include groups showing systematic shifts of alpha band activity, which consequently increases alpha band frequency ranges measurable in the overall study sample.

Such frequency shifts have been repeatedly reported in patients with hepatic encephalopathy (HE). HE describes changes in neurological function as a consequence of liver dysfunction (Häussinger and Schliess, 2008). This patient group is known to exhibit a global slowing of oscillatory activity (Kullmann et al., 2001; Timmermann et al., 2005; Olesen et al., 2011; Butz et al., 2013), with especially prominent effects found for the alpha band peak frequency (Kullmann et al., 2001; Marchetti et al., 2011; Olesen et al., 2011; Götz et al., 2013). In addition to alpha band peak frequency decreases, topographical changes of peak frequency generators have been repeatedly shown in HE patient samples. Early electrophysiological studies mention topographical shifts in peak frequency sources from the occipito-parietal to parieto-central areas (Sagalés et al. (1990), Kullmann et al. (2001), Montagnese et al. (2007), Olesen et al. (2011)). Although most of these results remain on the descriptive level, this repeatedly published effect has been labeled "anteriorization" of peak frequency activity. A recent MEG study likewise addressed this topic and reported a spatial blurring of oscillatory sources in HE patients compared to healthy controls (Götz et al., 2013).

HE patients also demonstrate a variety of neuropsychological impairments, including deficits in visual perception (Häussinger et al., 2007; Götz et al., 2013). These visual perceptual impairments are reflected in a decreased critical flicker frequency (CFF). The CFF assesses the temporal resolution of the visual sensory system by presenting a red light with an initial frequency of 60 Hz, which is gradually and linearly decreasing in frequency. While initially being perceived as a steady and continuous light, subjects indicate the time point at which they perceive the light as a discontinuous flicker (Kircheis et al., 2002). The CFF can be used to differentiate subclinical disease stages from overt clinical HE manifestation (Romero-Gómez et al., 2007; Sharma et al., 2007; Torlot et al., 2013) and further correlates with the disease severity in HE patients (Kircheis et al., 2002).

Regarding neurotransmitter concentration levels, HE patients show disease-related changes in γ-aminobutyric acid (GABA) levels. However, so far results have been inconsistent. Whereas classical theories advocated a generally increased GABAergic tone in HE patients (Schafer and Jones, 1982), recent studies put forward a more complex picture of regionally specific changes in GABA levels (e.g., Cauli et al., 2009a; Cauli et al., 2009b; Llansola et al., 2015). Moreover, our group reported a significant decrease in the occipital GABA-to-creatine ratio (GABA+/Cr) for HE patients compared to healthy controls (Oeltzschner et al., 2015). Although first investigations of healthy subjects have not demonstrated a relationship between occipital alpha band peak frequency and occipital GABA levels (Baumgarten et al., 2016), connections remain unknown for HE patients. Given such a connection, occipital GABA levels could represent a critical parameter linking disease-related changes in oscillatory activity and disease-related sensory impairments in HE.

The present study investigated the relationship between individual electrophysiological (occipital alpha band peak frequency), perceptual (CFF), and neurochemical (occipital GABA+/Cr levels) parameters in patients with varying grades of HE (minimal HE / manifest HE) and healthy controls. With this approach, we aimed to assess if neuronal oscillatory activity acts as a connecting factor between the perceptual visual sampling rate and occipital GABA+/Cr levels. By specifically including a patient sample for which perceptual impairments and regionally specific decreases in GABA+/Cr levels were known, the present investigation goes beyond previous studies, which examined only healthy subjects and only single connections (i.e., only the connection between alpha band peak frequency and CFF or GABA+/Cr levels). This way, the hypothesized connections can be tested within an increased parameter space of the investigated metrics, as compared to the investigation of healthy subjects alone. In accordance with previous findings (e.g., Kullmann et al., 2001; Olesen et al., 2011; Götz et al., 2013), we hypothesized that HE subjects demonstrate decreased occipital alpha band peak frequency and that this decrease worsens with progressing disease state. Given the comparatively high spatial resolution provided by MEG measures of neural activity, we additionally investigated if the topographical distribution of alpha band peak frequency differs between HE patients and healthy controls. Here, the main aim was to specify effects of peak frequency anteriorization previously reported by electroencephalographic studies. Further, we hypothesized a positive connection between occipital alpha band peak frequency and temporal visual perception as measured by the CFF in accordance with current models of perceptual cycles. Finally, we hypothesized that occipital alpha band peak frequency is correlated positively with occipital GABA+/Cr ratios.

Table 1
Demographic data for all participants separated by group. Data is presented as mean ± SD.

	Sex (male/female)	Age (years)	CFF (Hz)
Controls (n = 15)	7/8	59.9 ± 9.0	41.8 ± 4.1
mHE (n = 14)	9/5	53.6 ± 10.8	38.7 ± 4.0
HE1 (n = 14)	11/3	60.7 ± 7.3	35.7 ± 1.9

2. Materials & methods

2.1. Participants

43 participants (16 females, age: 58.1 ± 9.5 years (mean ± SD)) were included in the present study after providing prior written informed consent in accordance with the Declaration of Helsinki and the Ethical Committee of the Medical Faculty, Heinrich Heine University Düsseldorf (study number: 3644). The present sample was previously described in Oeltzschner et al. (2015). Specifically, 28 patients with hepatic encephalopathy (HE) and 15 healthy controls were included in the study (see Table 1 for demographic details of the respective groups). Patient inclusion criteria were a clinically confirmed liver cirrhosis and the diagnosis of either a minimal HE (mHE) or a clinically relevant HE (HE1; see below for the respective diagnosis criteria). The age-matched healthy participants were recruited as a control group. Data from all subjects (i.e., patients and healthy subjects) was used for the respective correlation analyses. All participants had normal or corrected to normal vision. Exclusion criteria for both patients and controls included severe intestinal, neurological, or psychiatric diseases excluding the diagnosis of HE for the patient group, the use of any medication acting on the central nervous system, blood clotting dysfunction, pregnancy, and diagnosed peripheral/retinal neuropathy. Further, patients had to confirm alcohol abstinence for at least 4 weeks prior to measurement. In addition, patients underwent a standard blood examination on the day of the measurement, which included an assessment of current blood alcohol levels.

Grading of HE disease severity consisted of a combination of the *West-Haven* criteria (Ferenci et al., 2002), the critical flicker frequency (CFF; Kircheis et al., 2002; Kircheis et al., 2014), a clinical assessment of the mental state and consciousness by an experienced clinician, and psychometric testing with the computer-based neuropsychological test battery from the Vienna Test System (Dr. Schuhfried GmbH, Mödling, Austria). Patients were classified as minimal HE when they did not exhibit manifest HE-related clinical symptoms but showed test score deviations of at least one standard deviation to the tests control cohort in more than two psychometric tests. CFFs were measured with a mobile measurement device, the HEPAtonorm™-Analyzer (nevoLAB, Maierhöfen, Germany). To assess the individual CFF, a flickering light is presented to the participants. The light starts to flicker with a frequency of 60 Hz, which is perceived as a continuous light. Then, the frequency by which the light flickers steadily decreases and participants are requested to report when they first perceive the light as clearly flickering, instead of a continuous light. Importantly, the CFF was shown to decrease depending on HE disease severity, with 39 Hz suggested as a cut-off to detect manifest HE patients (Kircheis et al., 2002; Kircheis et al., 2014). Individual CFFs were assessed on the day of the MEG/MRS measurement.

2.2. MEG Data

Individual magnetoencephalography (MEG) data was assessed on the same day as the respective individual CFF and magnetic resonance spectroscopy (MRS) data, whereas MEG measurements were always performed prior to MRS measurements to avoid contamination of the magnetic brain signal.

2.2.1. Paradigm

Participants were seated in the MEG. All visual stimuli were projected on a translucent screen (60 Hz refresh rate) positioned 57 cm in front of the participant. Neuromagnetic activity was recorded during two sessions with a respective duration of 5 min each. For the first session, participants were instructed to focus a dimmed fixation dot (0.5° diameter) presented in the center of the screen, subsequently labeled eyes-open condition (EO). In the second session, subjects were visually and verbally instructed to close their eyes but remain awake. This condition is labeled eyes-closed condition (EC). During both sessions, participants were instructed to relax and refrain from any additional cognitive or motor activity. The intention for recording neuromagnetic activity for both the EO and EC condition was that oscillatory alpha band power is known to be increased during eyes-closed conditions (Adrian and Matthews, 1934; Ahveninen et al., 2007). Based on this, we expected to be able to record alpha band peak frequency more robustly in the EC condition. Stimulus presentation was controlled using Presentation software (Neurobehavioral Systems, Albany, NY, USA).

2.2.2. Data recording and preprocessing

Continuous spontaneous neuromagnetic brain activity was recorded with a 306-channel whole head MEG system (Elekta Oy, Helsinki, Finland) including 102 magnetometers and 204 planar gradiometers (102 pairs of orthogonal gradiometers) at a sampling rate of 1 kHz. Unless stated otherwise, data analysis was restricted to the planar gradiometers. To account for an offline rejection of artifacts introduced by eye movements, additional electro-oculograms (EOGs) were recorded. Electrodes were applied above and below the left eye as well as on the outer canthi of each eye. In addition, an electro-cardiogram (ECG) was recorded for offline artifact rejection of cardiac artifacts with two electrodes placed on the left collarbone and the lowest left rib. Individual head position during the MEG measurement was assessed using four head position indication (HPI) coils placed at the subjects' forehead and behind both ears. To obtain individual full-brain high-resolution standard T_1-weighted structural magnetic resonance images, subjects were measured in a 3 T whole-body MRI scanner (Siemens MAGNETOM Trio A TIM System, Siemens Healthcare AG, Erlangen, Germany). Structural MRIs were aligned offline with the MEG coordinate system based on the HPI coils and prominent anatomical landmarks (nasion, left and right preauricular points).

Offline analysis of MEG data was performed using custom-made Matlab scripts (The Mathworks Inc., Natick/MA, USA) and the Matlab-based open source toolbox FieldTrip (http://www.fieldtriptoolbox.org/; Oostenveld et al., 2011). Continuous MEG data were separated into EO and EC epochs. To this end, each epoch was defined from 3 s after beginning of the respective condition to 3 s before the end of the respective condition. Subsequently, epochs were semi-automatically and visually inspected for artifacts caused by SQUID jumps, muscle activity, and eye movements. Corresponding artifacts were identified by means of a z-score based algorithm implemented in FieldTrip. Linear trends and the mean power of each epoch were removed from the respective data set. Data sets were band-pass filtered at 1 Hz to 200 Hz and power line noise components were removed by using a band-stop filter encompassing the 50 Hz, 100 Hz, and 150 Hz components. Data epochs were segmented into trials of 1 s duration, which were defined with a 0.25 s overlap. Excessively noisy channels and trials were then removed after visual inspection. Further removal of cardiac and eye-movement related artifacts was achieved by means of an independent component analysis (ICA). To this end, mutual information between the respective ICA components and the EOG and ECG data was computed (Liu et al., 2012; Abbasi et al., 2015). Components were sorted according to the level of mutual information and visually examined regarding the topography and time course. Those components that showed a high level of mutual information as well as topographies and time courses characteristic for eye-movement or cardiac activity were removed

manually. Subsequently, ICA data was back-projected to the channel level. Previously removed channels were reconstructed by an interpolation of neighboring channels. For the EO condition, 62.3 ± 8.6 s (mean ± SEM; range: 30.5–116.8 s)/20.4 ± 2.6% of the total EO recording (range: 10.0–38.3%) of data were removed due to artifact contamination in the control group. In the mHE group, 52.6 ± 6.2 s (21.2–90.8 s)/17.3 ± 2.0% (7.0–29.8%) were removed. In the HE1 group, 46.8 ± 4.8 s (12.7–86.4 s)/15.4 ± 1.6% (4.2–28.3%) were removed. For the EC condition, 65.3 ± 9.3 s (29.0–135.2 s)/22.1 ± 2.9% (9.8–45.8%) of data were removed in the control group. In the mHE group, 46.0 ± 4.9 s (20.5–86.6 s)/15.6 ± 1.7% (7.0–29.4%) were removed. In the HE1 group, 42.4 ± 4.4 s (21.4–75.9 s)/14.4 ± 1.4% (7.3–25.2%) were removed. On average, 322.2 ± 29.3 (mean ± SD) trials in the EO condition and 313.9 ± 28.5 in the EC condition entered subsequent analyses, which were performed separately for the EO and EC condition.

2.2.3. Peak frequency determination

Individual alpha band peak frequencies were determined by applying a frequency analysis on time series data. As we hypothesized that HE patients exhibit a reduced peak frequency (i.e., the peak frequency would be located in lower frequencies compared to healthy subjects), we chose a frequency range for analysis that is substantially broader than the classical alpha frequency band. Thus, we determined peak frequencies between 4 and 14 Hz, whereas the alpha band typically is defined between 7 and 14 Hz (e.g., Haegens et al., 2014). Single trials were zero-padded to a length of 10 s in order to achieve a frequency resolution of 0.1 Hz. Subsequently, a Fourier transformation with a single Hanning taper was applied for the entire trial duration. For each condition (i.e., EO, EC), spectral power was averaged over all trials for each frequency separately, independently for each of the 204 gradiometers. Subsequently, gradiometer pairs were combined by summing spectral power across each pair of orthogonal gradiometers, resulting in 102 channel pairs. Since the present study specifically investigates occipital alpha band activity, ten medial channel pairs covering the occipital cortex were selected for further processing (van Dijk et al., 2010; Fig. S1). Individual alpha-band peak frequencies were defined as those frequencies with maximal power between 4 and 14 Hz and detected by means of the Matlab function *'findpeaks.m'*. Additionally, the power value of a potential peak frequency had to exhibit an amplitude increase of at least 10% relative to neighboring peaks (i.e., the option *'MinPeakProminence'* was set to 10% of the respective peak amplitude; see also Baumgarten et al., 2017). By this, it was guaranteed that spontaneous power fluctuations and the 1/f power distribution would not be mistaken as frequency peaks and that selected peak frequencies would show a sufficient peak size relative to neighboring frequencies.

2.2.4. Source analysis

To localize the main source of the respective individual alpha band peak frequency, we calculated source-level power estimates using an adaptive spatial filtering technique (DICS; Gross et al., 2001). Therefore, a regular spaced 3D grid with 0.5 cm resolution was applied to the Montreal Neurological Institute (MNI) template brain. Subject-wise individual grids were computed by nonlinearly warping the subject-specific structural MRI on the MNI template gird and then applying the inverse of this warp to the MNI template grid. For each grid point, a lead-field matrix was computed using a realistically shaped single-shell volume conduction model (Nolte, 2003). The cross-spectral density (CSD) matrix was computed between all MEG gradiometer pairs for the respective individual sensor-level alpha band peak frequency by applying a Fourier transformation on the entire trial duration. For each individual grid point, spatial filters were constructed by using the CSD and lead-field matrix. CSD matrices of all single trials were then projected through these spatial filters and subsequently averaged across trials, resulting in across-trial-averages of estimated source power for the respective individual alpha band peak frequencies. To correct for differing signal-to-noise ratios across grid points, grid-point-specific source power estimates were divided by grid-point-specific noise estimates. The resulting individual peak frequency source power distributions were statistically compared across groups by means of a non-parametric randomization test (Maris and Oostenveld, 2007) implemented within the FieldTrip toolbox. To this end, peak frequency source power estimates were compared across groups with an independent samples F-test. F-values of spatially adjacent grid points exceeding an a priori-defined threshold ($p < 0.05$) were combined to a cluster and F-values within a cluster were summed up and entered in the second-level cluster statistic. Subsequently, a reference distribution was computed by randomly permuting the data, assuming no differences between groups and thus exchangeability of the data. Random assignments were repeated 1000 times, resulting in a summed cluster F-value for each repetition. The proportion of elements in the reference distribution exceeding the observed maximum cluster-level test statistic was used to derive a p-value for each cluster. Importantly, this approach effectively controls for the Type I error rate due to multiple comparisons.

2.3. Magnetic resonance spectroscopy data

Magnetic resonance spectroscopy (MRS) measures were performed on a clinical 3 T whole-body MRI scanner (Siemens MAGNETOM Trio A TIM System, Siemens Healthcare AG, Erlangen, Germany) using a 12-channel head matrix coil. For target volume localization and segmentation purposes, high-resolution 3D anatomical transversal T_1-weighted magnetization prepared gradient echo (MP RAGE) scans were performed (TR/TE = 1950/4.6 ms, FoV 256 × 192 mm, 256 × 192 matrix within-slice, 176 slices, slice thickness 1 mm, resulting in isotropic resolution of 1 mm). MRS data analyzed in the present study were computed for spectroscopic volumes placed in the central occipital lobe (please see Fig. 3A in Oeltzschner et al., 2015 for an exemplary spectroscopic volume placement). Volumes were manually aligned to include as much of the visual area as possible with caudal boundaries aligned along the *cerebellar tentorium*, while minimizing lipid contamination of the spectra by including portions of the skull in the volume. Subsequent to T_1-weighted planning sequences and the localization of the target volumes, MEGA PRESS (Mescher et al., 1998) spectra were acquired (number of excitations = 192, TR = 1500 ms, TE = 68 ms, V = 3 × 3 × 3 cm^3, bandwidth = 1200 Hz, 1024 data points). Editing of the spectra was conducted by J-refocusing pulses irradiated at 1.9 ppm ('On' resonance) and 7.5 ppm ('Off' resonance) using Gaussian pulses with a bandwidth of 44 Hz. In total, 192 averages (96 On spectra, 96 Off spectra) were acquired, resulting in a total measurement time of 4.8 min per session.

The MATLAB-based tool GANNET 2.0 (Edden et al., 2014) was used to process MRS spectral data. This postprocessing included individual frequency and phase correction of the single acquisitions. Fitting of the 3 ppm GABA resonance was performed in the frequency domain with a single Gaussian, whereas the 3 ppm creatine peak was modeled as a single Lorentzian peak. For subsequent analyses, the GABA-to-creatine ratio (GABA+/Cr) was used (see also Mullins et al., 2014; Oeltzschner et al., 2015).

2.4. Data analysis & statistical evaluation

To assess group level differences of alpha band peak frequency, CFF, and GABA+/Cr the following analysis steps were performed. Group level differences were investigated by means of a one-factor-repeated-measures ANOVA and post-hoc Tukey's range tests (i.e., a post-hoc *t*-tests correcting for the family-wise error-rate). Prior to computing the ANOVA, a Levene test was performed to ensure homoscedasticity. If no homoscedasticity was given, the robust Brown-Forsythe test was performed instead of an ANOVA. Furthermore, if a Shapiro-Wilk test indicated a departure from normality for the respective parameter, a non-

parametric Kruskal-Wallis test was computed instead of the one-factor-repeated-measures ANOVA, and Dunn-Bonferroni post-hoc tests were computed instead of post-hoc Tukey's range tests.

The present study aimed at elucidating connections between individual alpha band peak frequencies and different markers related to HE disease severity. To this end, individual alpha band peak frequencies of all participants (i.e., healthy controls and patients) were linearly correlated (Pearson) with the individual CFF measure and occipital GABA+/Cr levels. In order to compare correlation coefficients for the correlation between CFF and alpha band peak frequency in both EO and EC condition, we applied the Meng *Z*-test (Meng et al., 1992). However, certain parameters investigated in this study are known to be influenced by different demographic or measurement-related factors. For example, alpha band peak frequency is known to decrease with older age (Lindsley, 1939; Aurlien et al., 2004) and MRS derived GABA estimates vary depending on the amount of gray matter inclusion in the MRS voxel (Simister et al., 2003). Therefore, we accordingly corrected measures of correlation by computing partial correlations (Pearson) between alpha band peak frequency and CFF corrected for age. Further, the correlation between alpha band peak frequency and occipital GABA+/Cr was corrected for age and gray matter volume within the occipital MRS voxel. Previous analyses reported significant correlations between CFF and occipital GABA+/Cr ratios in the present data set (Oeltzschner et al., 2015). To determine if any potential correlation present between alpha-band peak frequency and occipital GABA+/Cr would be mediated only by the variance of the CFF values, we further corrected the correlation between alpha-band peak frequency and occipital GABA+/Cr for age, gray matter volume, and CFF. Correction for multiple comparisons was performed by means of the Benjamini-Hochberg method in order to control the false discovery rate at $Q = 0.05$. Statistical comparison of group level differences as well as correlation analyses were performed with SPSS Statistics 24.

3. Results

A summary of the measured target variables separated by group is presented in Table 2.

3.1. Alpha band peak frequencies

Alpha band peak frequencies could be successfully determined in 38 of 43 participants in the eyes-open (EO) condition and in 42 of 43 participants in the eyes-closed (EC) condition. Distribution of alpha band peak frequencies significantly deviated from normality only for the control group in the EC condition ($W(15) = 0.87$, $p < 0.05$). Thus, the group level comparison of mean alpha band peak frequencies in the EC condition was performed by means of a non-parametric Kruskal-Wallis test. For the EO condition, no significant deviations from homoscedasticity ($F(2,35) = 2.81$, $p = 0.07$) were observed. Group level average alpha band peak frequencies were significantly different for the EO condition ($F(2,35) = 9,37$, $p < 0.01$), with significant post-hoc differences between the control group and the mHE group ($p < 0.01$) and between the control group and the HE1 group ($p < 0.01$). Likewise, group level average alpha band peak frequencies also differed significantly for the EC condition ($\chi^2(2) = 15.4$, $p < 0.01$, with median peak frequencies of 9.8 (first quartile: 8.9 Hz, third quartile: 10.5 Hz) for controls, 8.6 (first quartile: 7.55 Hz, third quartile: 9.17 Hz) for mHE patients, and 8.2 (first quartile: 7.25 Hz, third quartile: 8.55 Hz) for HE1 patients; Fig. 1A), with significant post-hoc differences between the control group and the mHE group ($p < 0.05$) and between the control group and the HE1 group ($p < 0.01$).

3.2. Source level alpha band peak frequencies

Group-wise peak frequency source power distributions for the EO and the EC condition (Fig. 2) were displayed on the MNI template brain. Statistical comparison of peak frequency source power distributions across groups revealed no significant differences in source power distribution for the EO and the EC condition (all $p > 0.05$).

3.3. CFF

Visual temporal resolution as measured with the CFF could be successfully determined in all participants. For all groups, the distribution did not significantly deviate from normality ($p > 0.2$ for all groups). However, the variable CFF significantly deviated from homoscedasticity ($F = 4.41$, $p < 0.05$). Group level CFF significantly differed between groups ($F(2,32.3) = 11.12$, $p < 0.01$; Fig. 1B). Post-hoc tests showed significant differences between controls and HE1 patients ($p < 0.01$), a trend between controls and mHE patients ($p = 0.06$), and a trend between mHE patients and HE1 patients ($p = 0.07$).

3.4. GABA+/Cr levels

Occipital GABA+/Cr levels could be successfully determined in 40 of 43 participants. GABA+/Cr levels significantly differed from normal distribution for the mHE group ($W(12) = 0.8$, $p = 0.01$). Therefore, group level comparisons of GABA+/Cr levels were performed by means of a non-parametrical Kruskal-Wallis test. Group level GABA+/Cr levels significantly differed between groups ($\chi^2(2) = 15.1$, $p < 0.01$, with median GABA+/Cr levels of 0.108 for controls, 0.077 for mHE patients and 0.087 for HE1 patients; Fig. 1C). Post-hoc tests showed significant differences between controls and mHE patients ($p < 0.01$) as well as between controls and HE1 patients ($p < 0.01$).

3.5. Correlations

In order to investigate potential relations between occipital alpha band peak frequency (EO and EC), CFF, and occipital GABA+/Cr levels, we computed partial linear (Pearson) correlations. Correlations between alpha band peak frequency and CFF were corrected for age, whereas correlations between alpha band peak frequency and occipital GABA+/Cr levels were corrected for age and gray matter fraction within the occipital MRS voxel. Since a previous study found significant correlations between CFF and occipital GABA+/Cr levels in the present data set (Oeltzschner et al., 2015), we additionally corrected the correlation between alpha band peak frequency and occipital GABA+/Cr levels for CFF. Correction for multiple comparisons was performed by means of the Benjamini-Hochberg method, with both unadjusted and adjusted *p*-values provided subsequently.

A significant positive linear correlation between alpha band peak frequency and CFF was found for the EO condition ($r = 0.33$, $p < 0.05$, adjusted $p = 0.048$) and for the EC condition ($r = 0.49$, $p < 0.01$,

Table 2
Target variables separated by group. Data is presented as mean (median) ± SD.

	Age (years)	Alpha Band Peak Frequency – EO (Hz)	Alpha Band Peak Frequency – EC (Hz)	CFF (Hz)	GABA+/Cr Levels (a.u.)
Controls	59.9 (59.0) ± 9.0	9.9 (9.9) ± 0.9	9.5 (9.8) ± 1.2	41.8 (41) ± 4.1	0.107 (0.108) ± 0.011
mHE	53.6 (56.0) ± 10.8	8.5 (8.4) ± 1.2	8.4 (8.6) ± 0.9	38.7 (38.9) ± 4.0	0.088 (0.077) ± 0.026
HE1	60.7 (61.0) ± 7.3	8.5 (8.5) ± 0.7	7.9 (8.2) ± 1.1	35.7 (35.5) ± 1.9	0.084 (0.087) ± 0.011

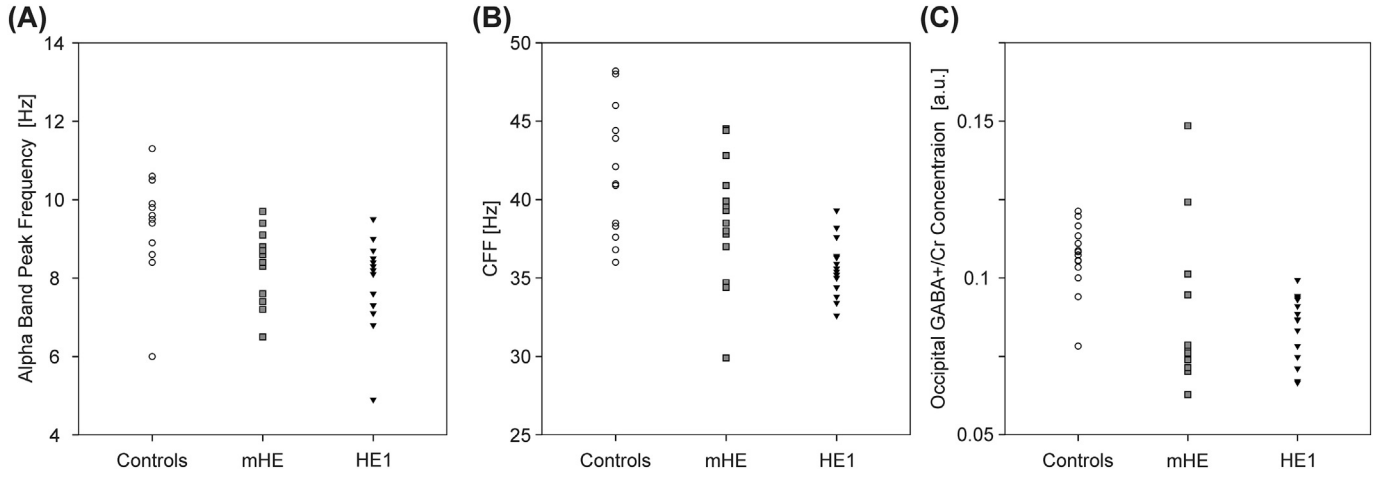

Fig. 1. Individual occipital alpha band peak frequencies in the eyes-closed (EC) condition (A), CFF (B) and occipital GABA+/Cr levels (C) separated by group. Each data point represents data for a single subject.

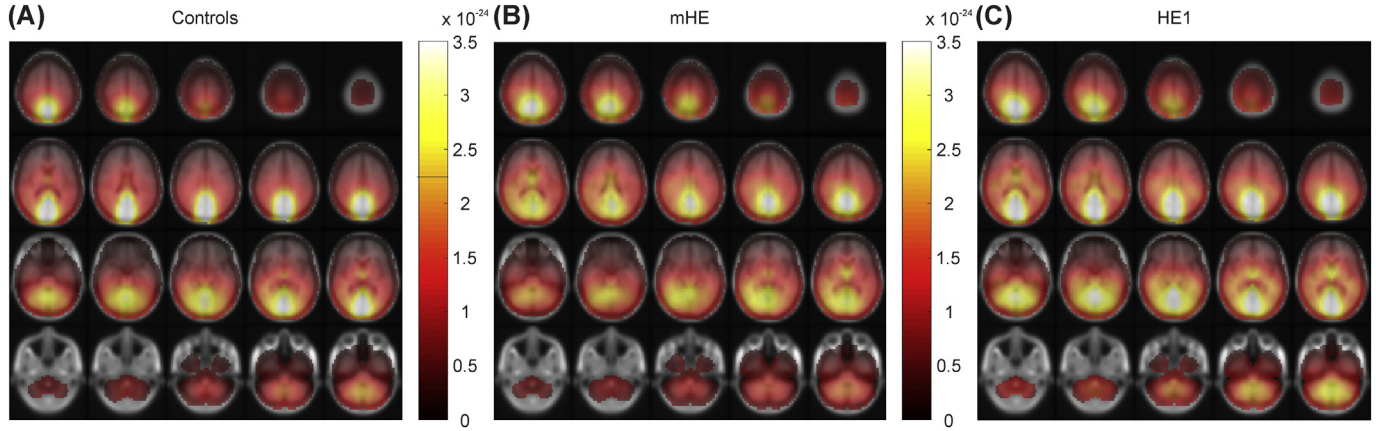

Fig. 2. Group-level average alpha band peak frequency source power distributions for the eyes-closed (EC) condition displayed on the MNI template brain for healthy controls (A), mHE patients (B), and HE1 patients (C). Source power estimates at each grid point are corrected for the noise estimate of the respective grid point (please see the Materials and methods part for further details). Color bars depict arbitrary units (a.u.) and uniformly apply to all three images.

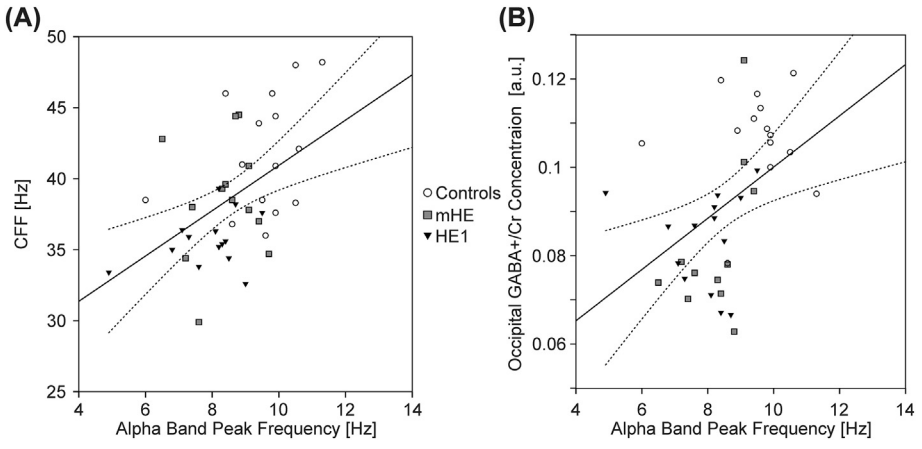

Fig. 3. Scatterplots for individual occipital alpha band peak frequency for the eyes-closed (EC) condition as a function of CFF (A) and occipital GABA+/Cr levels (B). Correlations between occipital alpha band peak frequency and CFF were corrected for age. Correlations between occipital alpha band peak frequency and occipital GABA+/Cr levels were corrected for age and gray matter volume within the occipital MRS voxel. Insets show the regression line (straight line) and the 95% confidence intervals for the mean (dotted lines).

adjusted p = 0.003; Fig. 3A). No significant difference was found comparing the correlation coefficients between CFF and alpha band peak frequency in the EO and the EC condition (z = 1.25, p = 0.1). For correlations between alpha band peak frequency and occipital GABA+/Cr levels, significant positive linear correlations were observed for the EO condition ($r = 0.55$, $p < 0.01$, adjusted p = 0.003) and the EC condition ($r = 0.44$, $p < 0.01$, adjusted p = 0.009; Fig. 3B). If CFF was included as an additional control variable, correlations remained significant for both the EO ($r = 0.5$, $p < 0.01$, adjusted p = 0.006) and the EC condition ($r = 0.34$, $p < 0.05$, adjusted p = 0.048).

4. Discussion

The present study investigated connections between occipital alpha band peak frequencies, visual temporal resolution assessed by means of the Critical Flicker Frequency (CFF), and occipital GABA-to-creatine

(GABA + /Cr) levels. In accordance with our hypothesis, patients with manifest HE (i.e., HE1 patients) showed a significant reduction in alpha band peak frequency (Fig. 1A), CFF (Fig. 1B), and occipital GABA + /Cr levels (Fig. 1C) compared to healthy controls. For patients with minimal HE (mHE), alpha band peak frequency and the occipital GABA + /Cr concentration but not CFF were significantly different from healthy controls. No significant changes between patient groups and healthy controls were found regarding the topographical distribution of the alpha band peak frequency sources. Further, we could determine positive linear correlations between alpha band peak frequency recorded for the eyes-open condition (EO) and eyes-closed condition (EC), and the CFF (Fig. 3A). Thus, subjects exhibiting a higher visual temporal resolution, also on average exhibited a higher alpha band peak frequency. Although correlation coefficients were higher for correlations between CFF and alpha band peak frequency in the EC condition compared to the EO condition, this difference was not significant. Presumably, the higher correlation coefficient for the EC condition can be explained by a higher signal-to-noise ratio for alpha band power during closing of the eyes (Adrian and Matthews, 1934; Ahveninen et al., 2007), which allows for a more robust peak frequency determination. Finally, significant positive linear correlations were also present between alpha band peak frequency recorded for both experimental conditions, and occipital GABA + /Cr levels (Fig. 3B). Here, individuals with higher occipital alpha band peak frequencies also on average possessed a higher occipital GABA + /Cr ratio.

Contrary to previous studies, no significant differences in CFF were found between both healthy controls and mHE patients, as well as between mHE patients and HE1 patients. Although at first glance these null findings might suggest a reduced sensitivity for the CFF parameter, we would like to highlight that the CFF has been repeatedly shown to be a sensitive and diagnostically valuable parameter to distinguish healthy individuals from those with pre-clinical forms of HE (e.g., Sharma et al., 2007), as well as to distinguish between different HE disease stages (Kircheis et al., 2002). Further support for this notion is provided by the comparatively large sample sizes provided by these studies (approx. 90–150 patients). Due to the extensive MEG and MRS measurements presented here, the present study was not able to include a patient sample of comparable size. Thus, we interpret the present null findings rather as an effect of low statistical power resulting from a limited sample size, instead of indicating low sensitivity of the CFF as diagnostic tool. In line with this, the present paper does not aim to promote peak frequency measurements in sensory cortices or local GABA + /Cr concentrations as a diagnostic marker superior to CFF. Despite the potential of peak frequency measurements and GABA + /Cr concentrations as an additional predictor of disease state, practical consideration in terms of measurement effort, time, and financial costs necessary to acquire these parameters have to be taken into account.

Although GABA + /Cr levels differed significantly between healthy controls and both patient groups, no significant difference could be found between mHE and HE1 patient groups. This might partially be due to the relatively high variance of GABA + /Cr levels in mHE patients. Presumably, the broad distribution of GABA + /Cr levels in mHE patients is a result of the rather coarse mHE diagnosis criteria, which is based on performance decreases in a specific number of different psychometrical tests. In contrast, HE1 categorization is based on more neuropsychiatric impairments (Ferenci et al., 2002). Since decreases in test performance represent a behavioral output measure, it can be assumed that such performance decreases can result from multiple different neuronal sources. Thus, GABA + /Cr levels might already be altered in some mHE patients, whereas other in mHE patients GABA + /Cr levels might be within the normal range, but test performance is impaired due to different factors. In addition, the present results are in agreement with an earlier MRS study investigating a large mHE sample (Singhal et al., 2010), which likewise reported substantially higher standard deviations for occipital GABA + /Cr levels in mHE patients compared to healthy controls.

Most studies assessing neurophysiological parameters in patient groups aim to operationalize the respective parameters as disease-specific diagnostic biomarker. Although this has previously been performed for peak frequencies in HE (e.g., Van der Rijt et al., 1984; Kullmann et al., 2001; Marchetti et al., 2011; Olesen et al., 2011; Schiff et al., 2016), this was not the primary intention of the present study. Rather, we wanted to investigate the connections between three different parameters (i.e., electrophysiological, perceptual, and neurochemical variables) connected by previous models of perceptual sampling and experimental evidence derived from both human and animal studies. By additionally including a patient group for which a general decrease of oscillatory frequency and perceptual sampling is well documented (see Butz et al., 2013 for a review on this topic), we were able to test the predictions about the connection between peak frequencies and visual perceptual sampling based on a broader distribution of the investigated parameters.

The present correlational results support a group-dependent effect. Significant correlations between alpha band peak frequency and CFF, as well as alpha band peak frequency and occipital GABA + /Cr levels were present when all participants (i.e., healthy individuals and patients) were analyzed. Additional analyses focusing solely on one specific group (i.e., separate analyses for the control, mHE, and HE1 group) yielded no significant results. Although the general consequence of a smaller sample size should be mentioned here, it is unlikely that smaller sample sizes are the only reason for the results. Rather, the results point in the direction that the respective correlations do not primarily rest on individual differences in the measured parameters, but more on differences between the groups. This interpretation is further supported by the distribution of the subsamples on the correlation plots (Fig. 3A, B). Instead of the majority of single subjects clustering on the linear regression line, rather the 3 different subsamples are located close to the linear fit, with the in-group subjects following a more random distribution. Notably, this finding stands in contrast to previous studies relating resting state peak frequency to CFF in HE patients (Götz et al., 2013; May et al., 2014). However, the study of May and colleagues assessed alpha band peak frequencies originated from the primary somatosensory cortex (May et al., 2014), thereby recording oscillatory activity from cortical regions not primarily associated with visual stimulus processing. Likewise, Götz and colleagues (Götz et al., 2013) used a spatially unspecific peak frequency determination without any spatial or sensor restrictions. Therefore, the analyzed peak frequencies might have originated from other cortical areas than the occipital cortex.

The finding of a correlation between occipital alpha band peak frequency and CFF across groups (instead of within groups) does not suggest that the individual occipital alpha band peak frequency precisely indicates the individual temporal visual resolution. In contrast, recent studies reported a correlation of individual alpha band peak frequency and temporal resolution of perception in healthy participants (Cecere et al., 2015; Samaha and Postle, 2015). However, these studies used a very different experimental approach along with substantially younger participants. Samaha and Postle (2015) tasked their participants to discriminate two spatially overlapping, successively flashing lights from a single flashing light, with the interstimulus interval between the two stimuli being determined by individual perceptual thresholds. In contrast, the present study presented subjects with a flickering light which steadily decreased in frequency, with subjects asked to indicate at which frequency they perceived the light as flickering (i.e., not as a continuously light). We point out that the paradigm used by Samaha and Postle assesses visual temporal perception in a more indirect way, i.e., by means of a comparison of flash durations. The CFF on the other hand aims to determine the frequency for which one perceives the light as flickering and non-continuous directly. Cecere et al. (2015) implemented a multimodal audio-visual integration task, with subjects performing the sound-induced double-flash illusion task. Here, subjects had to report if they perceived either one single or two

successive visual flashes, while a single flash was temporally paired with two auditory beeps presented at a different time delay. Although this paradigm likewise focusses on perceptual resolution, the approach is generally multimodal and thus focuses on the temporal binding of stimulation in different modalities. In addition, the samples of both studies consisted entirely of healthy and young participants. Although we corrected for the factor age by adding age as a covariate in the partial correlation, general age-related differences between the respective samples cannot be ruled out. For example, there are reports of alpha band peak frequencies shifting to more frontal positions with increasing age, whereas it is unknown if posterior alpha power is decreasing or frontal alpha power is increasing (Chiang et al., 2011). This shift in weight could result in the measurement of different generators of alpha power activity for samples of young and old age, which could not be compensated by partial correlation.

The first main result that the correlation between alpha band peak frequency and CFF were mainly driven by group differences merits further discussion. Although it currently remains unclear how alpha band peak frequency, visual perceptual sampling, and local GABAergic activity are interlinked, we provide a short speculation on potentially underlying mechanisms. The connection between visual temporal resolution and alpha band activity can be explained by current models of perceptual cycles (Vanrullen and Koch, 2003; Baumgarten et al., 2015; Vanrullen, 2016). Here, ongoing neuronal oscillations in sensory cortices constitute an electrophysiological correlate of perceptual windows. It is hypothesized that multiple temporally distinct stimuli that fall within such a single window are fused and thus perceived as single percept. In contrast, if multiple temporally distinct stimuli fall within two distinct perceptual windows, they are perceived as two temporally distinct percepts. Probabilities for multiple temporally distinct stimuli to either fall within one or two cycles are determined by both the temporal distance between the distinct stimuli and the cycle length of the neuronal oscillation. The respective cycle length is directly related to the frequency of the ongoing neuronal oscillation. Given the definition of peak frequency as the local power dominant frequency, peak frequencies index the current cycle length of ongoing oscillatory activity, by which the length of a perceptual window can be inferred. Thus, a higher peak frequency indexes a shorter cycle length, which in turn points towards a higher perceptual resolution and a denser perceptual sampling. Since an exact individual mapping between peak frequency and perceptual resolution was not found, the present results indicate a rather coarse and stochastic connection between occipital alpha peak frequency and visual temporal resolution. In addition, it has to be taken into account that HE goes along with multiple other symptoms which potentially impede CFF performance. Thus, although CFF reliably indexes disease severity in HE patients, there presumably are also other factors besides alpha band activity which contribute to impairments in visual temporal resolution. For example, flexible deployment of attention and underlying gamma band activity have been reported to be impaired in HE patients. Importantly, these impairments were likewise related to visual temporal resolution as measured by CFF (Kahlbrock et al., 2012).

The second main finding of the present study is a significant positive linear correlation between occipital alpha band peak frequencies and occipital GABA+/Cr levels. Similar to the correlation between alpha band peak frequency and CFF, connections seem to rely mostly on the group level and not on the individual level. In general, the inhibitory effects mediated by GABAergic interneurons are thought essential for the rigid temporal coding necessary for the generation of oscillatory neuronal activity (Lozano-Soldevilla et al., 2014). So far, individual occipital GABA levels have been mostly related to frequencies within the gamma band (Bartos et al., 2007). For example, Muthukumaraswamy et al. (2009) reported a positive connection between occipital GABA+/Cr and occipital gamma peak frequency (but see Cousijn et al., 2014 for a contradictory finding). Balz et al. (2016) reported connections between GABA levels in the superior temporal sulcus as measured by MRS and oscillatory gamma band power. Importantly, GABA levels also correlated with the perceptual parameters in an audiovisual perception task. In contrast, the connection between oscillatory alpha band activity and occipital GABA+/Cr levels remains speculative. Animal studies suggest that phasic GABAergic inhibition temporally shapes the output of thalamocortical neurons, which in turn is deemed crucial for discretely constraining the temporal neuronal activity within occipital cortex areas and thus influences the processing of low-level visual information (Lőrincz et al., 2009). In humans, a reasonable number of studies show effects of pharmacological GABAergic modulation on occipital oscillatory alpha band activity (e.g., Schreckenberger et al., 2004; Ahveninen et al., 2007). However, these studies almost exclusively focus on oscillatory power (reviewed by Lozano-Soldevilla, 2018), whereas modulations of peak frequency are rarely reported (but see Liley et al., 2003). Mechanistic models of thalamic generators driving the frequency of cortical alpha band activity by means of GABA-mediated conductance changes at 10 Hz have been recently put forward and related to visual stimulus processing (Gips et al., 2016). Here, multiple cycles of gamma band activity locked to alpha band phase are interpreted as a mechanism of temporal structuring for visual stimulus information, which relates to the abovementioned concept of perceptual cycles. Alpha band activity is seen as a mechanism of pulsed physiological inhibition, which separates incoming stimulus information in discrete sequential cycles. However, the location of GABAergic inhibition in this model lies within the thalamus, whereas the present study estimated GABA+/Cr levels in occipital cortical areas. Given the evidence of changes within the thalamocortical network connections due to GABAergic manipulation (Schreckenberger et al., 2004), it can be assumed that disease-related GABAergic concentration imbalances between these regions could critically affect the generation of alpha band oscillations, including shifts in peak frequency. Nonetheless, to obtain a clearer picture of the GABAergic influence on peak frequencies in sensory cortices, novel studies focusing specifically on this topic are necessary. Here, either human EEG/MEG studies investigating pharmacodynamical effects of GABAergic modulators on peak frequency changes in sensory cortices or animal studies directly investigating effects of GABAergic modulators on the presumed thalamo-cortical connection would be specifically valuable.

Nonetheless, it has to be kept in mind that GABA measurements by means of MRS can be considered a relatively coarse estimate of neurochemical concentrations. This owes to the relatively large voxel size, as well as to the inability to differentiate between synaptic and extrasynaptic GABA concentrations (Stagg, 2014). While the extracellular synaptic GABA levels are the most relevant to neurotransmission, MRS generally measures the total bulk tissue content of a metabolite, and therefore rather reflects the general GABAergic tone (Rae, 2014). As a quantitative measure of the local ability to exert and maintain inhibitory activity, GABA MRS levels are nevertheless of high functional relevance, and have been associated with numerous indicators of behavior and brain function (see e.g., Puts and Edden, 2012 for an overview).

The present findings of decreased alpha band peak frequencies in HE patients can further be related to reported changes in resting state functional connectivity within this patient group. A common result emerging from this line of research is the decline in clustering of functional nodes and an increased randomness in the topography of functional networks, which progressively worsens with increasing disease level (Jao et al., 2015). Specific functional connectivity decreases located in visual sensory areas for HE patients compared to healthy controls were recently reported by Zhang and colleagues (Zhang et al., 2017). Given that multiple theories presume functional integration between different cortex areas by means of alpha band synchronization (e.g., Jensen et al., 2012) and recent experimental evidence demonstrates top-down mediated alpha band phase adjustment between frontal and visual cortex areas (Solís-Vivanco et al., 2018), this suggests

that disease-related alterations in alpha band activity could be closely related to the broadly replicated changes of functional activity in HE. However, a direct connection between decreases in local oscillatory alpha band peak frequency and functional connectivity decreases in visual sensory areas remains to be shown in HE patients.

The present study found no significant differences in the topographical distribution of the alpha band peak frequency sources. Although multiple previous studies reported a general anteriorization of alpha band peak frequencies in HE patient samples (Sagalés et al. (1990), Kullmann et al. (2001), Montagnese et al. (2007), Olesen et al. (2011)), most of these studies only provided descriptive evidence without further statistical analysis. The present source distributions suggest alpha peak frequency sources to be more focally centered in the occipital cortex in healthy controls compared to both HE patient groups (Fig. 2). This would be in accordance with a recent MEG study (Götz et al., 2013), which similarly mentioned a spatial blurring of oscillatory sources in HE patients compared to healthy controls.

The broad distribution of alpha band peak frequencies might be considered a potential shortcoming of the present study, in the sense that the question arises if we really assessed peak frequencies for the alpha band in all participants. However, despite the significant differences in the mHE and HE1 samples, it can be safely assumed that our analysis approach yielded a reliable assessment of alpha band peak frequencies. First, the determined peak frequencies in the patient sample consisted of clearly discernible occipital frequency peaks (Fig. S2) present at rest (i.e., during the EO/EC condition), which supports the view that these peaks resemble the classical alpha band peak, albeit with decreased frequency. Further, alpha band peak frequency significantly differed depending on experimental condition (i.e., EO vs. EC, $t(37) = 2.14$, $p < 0.05$) and could be determined more reliably and in more subjects in the EC condition, which also represents a characteristic of the classical alpha rhythm (Berger, 1929; Götz et al., 2013).

Taken together, the present study demonstrates a connection between occipital alpha band peak frequency and temporal visual resolution as measured with the CFF. This connection is determined on group level (i.e., across subsamples) and not on the single subject level. Consequently, occipital alpha band activity does not seem to indicate the individual perceptual resolution, but rather seems to be decisively altered across varying disease stages of HE. The same holds true for the connection between occipital alpha band peak frequency and occipital GABA+/Cr levels. Thus, the present study reveals functional connections between electrophysiological, perceptual and neurochemical variables, with disease-related alterations in these variables declining in parallel.

Funding

This work was supported by the German Research Foundation [Sonderforschungsbereich (SFB) 974 Project B07]. This project has received funding from the European Union's Horizon 2020 research and innovation programme under the Marie Sklodowska-Curie grant agreement No 795998 (MSCA-IF-GF awarded to T.J.B.). The funding sources had no involvement in the study design, collection, analysis, and interpretation of the presented data.

Conflict of interest

G.K. and D.H. belong to a group of patent holders for the bedside measurement device determining the critical flicker frequency.

Acknowledgements

The authors would like to express their gratitude to Erika Rädisch (Department of Diagnostic and Interventional Radiology, University Hospital Düsseldorf) for support with MR measurements and to Dr. Nienke Hoogenboom for her help with the MEG measurements.

Appendix A. Supplementary data

Supplementary data to this article can be found online at https://doi.org/10.1016/j.nicl.2018.08.013.

References

Abbasi, O., Dammers, J., Arrubla, J., Warbrick, T., Butz, M., Neuner, I., Shah, N.J., 2015. Time-frequency analysis of resting state and evoked EEG data recorded at higher magnetic fields up to 9.4T. J. Neurosci. Methods 255, 1–11.

Adrian, E.D., Matthews, B.H., 1934. The Berger rhythm: potential changes from the occipital lobes in man. Brain 57, 355–385.

Ahveninen, J., Lin, F.H., Kivisaari, R., Autti, T., Hämäläinen, M., Stufflebeam, S., Belliveau, J.W., Kähkönen, S., 2007. MRI-constrained spectral imaging of benzodiazepine modulation of spontaneous neuromagnetic activity in human cortex. NeuroImage 35, 577–582.

Aurlien, H., Gjerde, I., Aarseth, J., Eldøen, G., Karlsen, B., Skeidsvoll, H., Gilhus, N., 2004. EEG background activity described by a large computerized database. Clin. Neurophysiol. 115, 665–673.

Balz, J., Keil, J., Roa Romero, Y., Mekle, R., Schubert, F., Aydin, S., Ittermann, B., Gallinat, J., Senkowski, D., 2016. GABA concentration in superior temporal sulcus predicts gamma power and perception in the sound-induced flash illusion. NeuroImage 125, 724–730.

Bartos, M., Vida, I., Jonas, P., 2007. Synaptic mechanisms of synchronized gamma oscillations in inhibitory interneuron networks. Nat. Rev. Neurosci. 8, 45.

Baumgarten, T.J., Schnitzler, A., Lange, J., 2015. Beta oscillations define discrete perceptual cycles in the somatosensory domain. Proc. Natl. Acad. Sci. 112, 12187–12192.

Baumgarten, T.J., Oeltzschner, G., Hoogenboom, N., Wittsack, H.-J., Schnitzler, A., Lange, J., 2016. Beta peak frequencies at rest correlate with endogenous GABA+/Cr concentrations in sensorimotor cortex areas. PLoS One 11, e0156829.

Baumgarten, T.J., Königs, S., Schnitzler, A., Lange, J., 2017. Subliminal stimuli modulate somatosensory perception rhythmically and provide evidence for discrete perception. Sci. Rep. 7.

Berger, H., 1929. Über das Elektrenkephalogramm des Menschen. Archiv. für. Psychiatrie und Nervenkrankheiten 87, 527–570.

Bollimunta, A., Mo, J., Schroeder, C.E., Ding, M., 2011. Neuronal mechanisms and attentional modulation of Corticothalamic alpha oscillations. J. Neurosci. 31, 4935–4943.

Busch, N.A., Dubois, J., Vanrullen, R., 2009. The phase of ongoing EEG oscillations predicts visual perception. J. Neurosci. 29, 7869–7876.

Butz, M., May, E.S., Häussinger, D., Schnitzler, A., 2013. The slowed brain: cortical oscillatory activity in hepatic encephalopathy. Hepatic Encephalopathy 536, 197–203.

Buzsáki, G., Draguhn, A., 2004. Neuronal oscillations in cortical networks. Science 304, 1926–1929.

Buzsáki, G., Watson, B.O., 2012. Brain rhythms and neural syntax: implications for efficient coding of cognitive content and neuropsychiatric disease. Dialogues Clin. Neurosci. 14, 345–367.

Cauli, O., Mansouri, M.T., Agusti, A.,Felipo, V., 2009a. Hyperammonemia increases GABAergic tone in the cerebellum but decreases it in the rat cortex. Gastroenterology 136, 1359–1367.e2.

Cauli, O., Rodrigo, R., Llansola, M., Montoliu, C., Monfort, P., Piedrafita, B., el Mlili, N., Boix, J., Agustí, A., Felipo, V., 2009b. Glutamatergic and gabaergic neurotransmission and neuronal circuits in hepatic encephalopathy. Metab. Brain Dis. 24, 69–80.

Cecere, R., Rees, G., Romei, V., 2015. Individual differences in alpha frequency drive crossmodal illusory perception. Curr. Biol. 25, 231–235.

Chakravarthi, R., Vanrullen, R., 2012. Conscious updating is a rhythmic process. Proc. Natl. Acad. Sci. 109, 10599–10604.

Chiang, A., Rennie, C.J., Robinson, P.A., van Albada, S.J., Kerr, C.C., 2011. Age trends and sex differences of alpha rhythms including split alpha peaks. Clin. Neurophysiol. 122, 1505–1517.

Cousijn, H., Haegens, S., Wallis, G., Near, J., Stokes, M.G., Harrison, P.J., Nobre, A.C., 2014. Resting GABA and glutamate concentrations do not predict visual gamma frequency or amplitude. Proc. Natl. Acad. Sci. 111, 9301–9306.

der Rijt, Van, Carin, C.D., Schalm, S.W., de Groot, G.H., de Vlieger, M., 1984. Objective measurement of hepatic encephalopathy by means of automated EEG analysis. Electroencephalogr. Clin. Neurophysiol. 57, 423–426.

Dugué, L., Marque, P., Vanrullen, R., 2011. The phase of ongoing oscillations mediates the causal relation between brain excitation and visual perception. J. Neurosci. 31, 11889.

Edden, R.A., Puts, N.A., Harris, A.D., Barker, P.B., Evans, C.J., 2014. Gannet: a batch-processing tool for the quantitative analysis of gamma-aminobutyric acid-edited MR spectroscopy spectra. J. Magn. Reson. Imaging 40, 1445–1452.

Engel, A.K., Fries, P., Singer, W., 2001. Dynamic predictions: oscillations and synchrony in top-down processing. Nat. Rev. Neurosci. 2, 704–716.

Ferenci, P., Lockwood, A., Mullen, K., Tarter, R., Weissenborn, K., Blei, A.T., 2002. Hepatic encephalopathy—definition, nomenclature, diagnosis, and quantification: final report of the working party at the 11th world congresses of gastroenterology, Vienna, 1998. Hepatology 35, 716–721.

Gips, B., Eerden, J.P., Jensen, O., 2016. A biologically plausible mechanism for neuronal coding organized by the phase of alpha oscillations. Eur. J. Neurosci. 44, 2147–2161.

Götz, T., Huonker, R., Kranczioch, C., Reuken, P., Witte, O.W., Günther, A., Debener, S., 2013. Impaired evoked and resting-state brain oscillations in patients with liver cirrhosis as revealed by magnetoencephalography. NeuroImage 2, 873–882.
Gross, J., Kujala, J., Hamalainen, M., Timmermann, L., Schnitzler, A., Salmelin, R., 2001. Dynamic imaging of coherent sources: studying neural interactions in the human brain. Proc. Natl. Acad. Sci. 98, 694–699.
Haegens, S., Cousijn, H., Wallis, G., Harrison, P.J., Nobre, A.C., 2014. Inter- and intra-individual variability in alpha peak frequency. NeuroImage 92, 46–55.
Hanslmayr, S., Aslan, A., Staudigl, T., Klimesch, W., Herrmann, C.S., Bäuml, K.-H., 2007. Prestimulus oscillations predict visual perception performance between and within subjects. NeuroImage 37, 1465–1473.
Hari, R., Salmelin, R., Mäkelä, J.P., Salenius, S., Helle, M., 1997. Magnetoencephalographic cortical rhythms. Int. J. Psychophysiol. 26, 51–62.
Häussinger, D., Schliess, F., 2008. Pathogenetic mechanisms of hepatic encephalopathy. Gut 57, 1156–1165.
Häussinger, D., Blei, A.T., Rodes, J., Benhamou, J.P., Reichen, J., Rizzetto, M., 2007. The Textbook of Hepatology: From Basic Science to Clinical Practise. Wiley-Blackwell, Oxford.
Hipp, J.F., Engel, A.K., Siegel, M., 2011. Oscillatory synchronization in large-scale cortical networks predicts perception. Neuron 69, 387–396.
Hubel, D.H., Wiesel, T.N., 1965. Receptive fields and functional architecture in two nonstriate visual areas (18 and 19) of the cat. J. Neurophysiol. 28, 229.
Jao, T., Schröter, M., Chen, C.L., Cheng, Y.F., Lo, C.Y.Z., Chou, K.H., Patel, A.X., Lin, W.C., Lin, C.P., Bullmore, E.T., 2015. Functional brain network changes associated with clinical and biochemical measures of the severity of hepatic encephalopathy. NeuroImage 122, 332–344.
Jensen, O., Bonnefond, M., Vanrullen, R., 2012. An oscillatory mechanism for prioritizing salient unattended stimuli. Trends Cogn. Sci. 16, 200–206.
Kahlbrock, N., Butz, M., May, E.S., Brenner, M., Kircheis, G., Häussinger, D., Schnitzler, A., 2012. Lowered frequency and impaired modulation of gamma band oscillations in a bimodal attention task are associated with reduced critical flicker frequency. NeuroImage 61, 216–227.
Kircheis, G., Wettstein, M., Timmermann, L., Schnitzler, A., Häussinger, D., 2002. Critical flicker frequency for quantification of low-grade hepatic encephalopathy. Hepatology 35, 357–366.
Kircheis, G., Hilger, N.,Häussinger, D., 2014. Value of critical flicker frequency and psychometric hepatic encephalopathy score in diagnosis of low-grade hepatic encephalopathy. Gastroenterology 146, 961–969.e11.
Kullmann, F., Hollerbach, S., Lock, G., Holstege, A., Dierks, T., Schölmerich, J., 2001. Brain electrical activity mapping of EEG for the diagnosis of (sub) clinical hepatic encephalopathy in chronic liver disease. Eur. J. Gastroenterol. Hepatol. 13, 513–522.
Liley, D.T., Cadusch, P.J., Gray, M., Nathan, P.J., 2003. Drug-induced modification of the system properties associated with spontaneous human electroencephalographic activity. Phys. Rev. E 68, 051906.
Lindsley, D.B., 1939. A longitudinal study of the occipital alpha rhythm in normal children: frequency and amplitude standards. Pedagogical Seminary J. Genet. Psychol. 55, 197–213.
Liu, Z., de Zwart, J.A., van Gelderen, P., Kuo, L.-W., Duyn, J.H., 2012. Statistical feature extraction for artifact removal from concurrent fMRI-EEG recordings. NeuroImage 59, 2073–2087.
Llansola, M., Montoliu, C., Agusti, A., Hernandez-Rabaza, V., Cabrera-Pastor, A., Gomez-Gimenez, B., Malaguarnera, M., Dadsetan, S., Belghiti, M., Garcia-Garcia, R., Balzano, T., 2015. Interplay between glutamatergic and GABAergic neurotransmission alterations in cognitive and motor impairment in minimal hepatic encephalopathy. Neurochem. Int. 88, 15–19.
Lőrincz, M.L., Kékesi, K.A., Juhász, G., Crunelli, V., Hughes, S.W., 2009. Temporal framing of thalamic relay-mode firing by phasic inhibition during the alpha rhythm. Neuron 63, 683–696.
Lozano-Soldevilla, D., 2018. On the physiological modulation and potential mechanisms underlying Parieto-occipital alpha oscillations. Front. Comput. Neurosci. 12, 23.
Lozano-Soldevilla, D., ter Huurne, N., Cools, R., Jensen, O., 2014. GABAergic modulation of visual gamma and alpha oscillations and its consequences for working memory performance. Curr. Biol. 24, 2878–2887.
Marchetti, P., D'Avanzo, C., Orsato, R., Montagnese, S., Schiff, S., Kaplan, P.W., Piccione, F., Merkel, C., Gatta, A., Sparacino, G., Toffolo, G.M., Amodio, P., 2011. Electroencephalography in patients with cirrhosis. Gastroenterology 141, 1680–1689.e2.
Maris, E., Oostenveld, R., 2007. Nonparametric statistical testing of EEG- and MEG-data. J. Neurosci. Methods 164, 177–190.
Mathewson, K.E., Gratton, G., Fabiani, M., Beck, D.M., Ro, T., 2009. To see or not to see: prestimulus alpha phase predicts visual awareness. J. Neurosci. 29, 2725–2732.
May, E.S., Butz, M., Kahlbrock, N., Brenner, M., Hoogenboom, N., Kircheis, G., Häussinger, D., Schnitzler, A., 2014. Hepatic encephalopathy is associated with slowed and delayed stimulus-associated somatosensory alpha activity. Clin. Neurophysiol. 125, 2427–2435.
Meng, X.L., Rosenthal, R., Rubin, D.B., 1992. Comparing correlated correlation coefficients. Psychol. Bull. 111, 172–175.
Mescher, M., Merkle, H., Kirsch, J., Garwood, M., Gruetter, R., 1998. Simultaneous in vivo spectral editing and water suppression. NMR Biomed. 11, 266–272.
Montagnese, S., Jackson, C., Morgan, M.Y., 2007. Spatio-temporal decomposition of the electroencephalogram in patients with cirrhosis. J. Hepatol. 46, 447–458.
Mullins, P.G., McGonigle, D.J., O'Gorman, R.L., Puts, N.A., Vidyasagar, R., Evans, C.J., Edden, R.A., 2014. Current practice in the use of MEGA-PRESS spectroscopy for the detection of GABA. NeuroImage 86, 43–52.
Muthukumaraswamy, S.D., Edden, R.A., Jones, D.K., Swettenham, J.B., Singh, K.D., 2009. Resting GABA concentration predicts peak gamma frequency and fMRI amplitude in response to visual stimulation in humans. Proc. Natl. Acad. Sci. 106, 8356–8361.
Nolte, G., 2003. The magnetic lead field theorem in the quasi-static approximation and its use for magnetoencephalography forward calculation in realistic volume conductors. Phys. Med. Biol. 48, 3637.
Oeltzschner, G., Butz, M., Baumgarten, T., Hoogenboom, N., Wittsack, H.-J., Schnitzler, A., 2015. Low visual cortex GABA levels in hepatic encephalopathy: links to blood ammonia, critical flicker frequency, and brain osmolytes. Metab. Brain Dis. 1–10.
Olesen, S.S., Graversen, C., Hansen, T.M., Blauenfeldt, R.A., Hansen, J.B., Steimle, K., Drewes, A.M., 2011. Spectral and dynamic electroencephalogram abnormalities are correlated to psychometric test performance in hepatic encephalopathy. Scand. J. Gastroenterol. 46, 988–996.
Oostenveld, R., Fries, P., Maris, E., Schoffelen, J.-M., 2011. FieldTrip: open source software for advanced analysis of MEG, EEG, and invasive electrophysiological data. Comput. Intell. Neurosci. 2011, 9.
Puts, N.A., Edden, R.A., 2012. In vivo magnetic resonance spectroscopy of GABA: a methodological review. Prog. Nucl. Magn. Reson. Spectrosc. 60, 29.
Rae, C., 2014. A guide to the metabolic pathways and function of metabolites observed in human brain 1H magnetic resonance spectra. Neurochem. Res. 39, 1–36.
Romei, V., Gross, J., Thut, G., 2010. On the role of Prestimulus alpha rhythms over Occipito-parietal areas in visual input regulation: correlation or causation? J. Neurosci. 30, 8692.
Romero-Gómez, M., Córdoba, J., Jover, R., del Olmo, J.A., Ramírez, M., Rey, R., de Madaria, E., Montoliu, C., Nuñez, D., Flavia, M., Compañy, L., Rodrigo, J.M., Felipo, V., 2007. Value of the critical flicker frequency in patients with minimal hepatic encephalopathy. Hepatology 45, 879–885.
Sagalés, T., Gimeno, V., de la Calzada, M.D., Casellas, F., Dolors Macià, M., Villar Soriano, M., 1990. Brain mapping analysis in patients with hepatic encephalopathy. Brain Topogr. 2, 221–228.
Samaha, J., Postle, B.R., 2015. The speed of alpha-band oscillations predicts the temporal resolution of visual perception. Curr. Biol. 25, 2985–2990.
Schafer, D., Jones, E.A., 1982. Hepatic encephalopathy and the γ-aminobutyric-acid neurotransmitter system. Lancet 319, 18–20.
Schiff, S., Casa, M., Di Caro, V., Aprile, D., Spinelli, G., de Rui, M., Angeli, P., Amodio, P., Montagnese, S., 2016. A low-cost, user-friendly electroencephalographic recording system for the assessment of hepatic encephalopathy. Hepatology 63, 1651–1659.
Schreckenberger, M., Lange-Asschenfeld, C., Lochmann, M., Mann, K., Siessmeier, T., Buchholz, H.G., Bartenstein, P., Gründer, G., 2004. The thalamus as the generator and modulator of EEG alpha rhythm: a combined PET/EEG study with lorazepam challenge in humans. NeuroImage 22, 637–644.
Sharma, P., Sharma, B.C., Puri, V., Sarin, S.K., 2007. Critical flicker frequency: diagnostic tool for minimal hepatic encephalopathy. J. Hepatol. 47, 67–73.
Simister, R.J., McLean, M.A., Barker, G.J., Duncan, J.S., 2003. A proton magnetic resonance spectroscopy study of metabolites in the occipital lobes in epilepsy. Epilepsia 44, 550–558.
Singer, W., Lazar, A., 2016. Does the cerebral cortex exploit high-dimensional, non-linear dynamics for information processing? Front. Comput. Neurosci. 10, 99.
Singhal, A., Nagarajan, R., Hinkin, C.H., Kumar, R., Sayre, J., Elderkin-Thompson, V., Huda, A., Gupta, R.K., Han, S.H., Thomas, M.A., 2010. Two-dimensional MR spectroscopy of minimal hepatic encephalopathy and neuropsychological correlates in vivo. J. Magn. Reson. Imaging 32, 35–43.
Solís-Vivanco, R., Jensen, O., Bonnefond, M., 2018. Top–down control of alpha phase adjustment in anticipation of temporally predictable visual stimuli. J. Cogn. Neurosci. 1–13.
Stagg, C.J., 2014. Magnetic resonance spectroscopy as a tool to study the role of GABA in motor-cortical plasticity. NeuroImage 86, 19–27.
Thorpe, S., Fize, D., Marlot, C., 1996. Speed of processing in the human visual system. Nature 381, 520–522.
Timmermann, L., Butz, M., Gross, J., Kircheis, G., Häussinger, D., Schnitzler, A., 2005. Neural synchronization in hepatic encephalopathy. Metab. Brain Dis. 20, 337–346.
Torlot, F.J., McPhail, M.J.W., Taylor-Robinson, S.D., 2013. Meta-analysis: the diagnostic accuracy of critical flicker frequency in minimal hepatic encephalopathy. Aliment. Pharmacol. Ther. 37, 527–536.
van Dijk, H., Schoffelen, J.-M., Oostenveld, R., Jensen, O., 2008. Prestimulus oscillatory activity in the alpha band predicts visual discrimination ability. J. Neurosci. 28, 1816–1823.
van Dijk, H., van der Werf, J., Mazaheri, A., Medendorp, W.P., Jensen, O., 2010. Modulations in oscillatory activity with amplitude asymmetry can produce cognitively relevant event-related responses. Proc. Natl. Acad. Sci. 107, 900–905.
Vanrullen, R., 2016. Perceptual cycles. Trends Cogn. Sci. 20, 723–735.
Vanrullen, R., Koch, C., 2003. Is perception discrete or continuous? Trends Cogn. Sci. 7, 207–213.
Vanrullen, R., Zoefel, B., Ilhan, B., 2014. On the cyclic nature of perception in vision versus audition. Philosophical transactions of the royal society of London. Series B. Biol. Sci. 369, 20130214.
Varela, F.J., Toro, A., John, E.R., Schwartz, E.L., 1981. Perceptual framing and cortical alpha rhythm. Neuropsychologia 19, 675–686.
Vijayan, S., Kopell, N.J., 2012. Thalamic model of awake alpha oscillations and implications for stimulus processing. Proc. Natl. Acad. Sci. 109, 18553–18558.
Zhang, G., Cheng, Y., Liu, B., 2017. Abnormalities of voxel-based whole-brain functional connectivity patterns predict the progression of hepatic encephalopathy. Brain Imaging Behav. 11, 784–796.